Weighted least square based lowrank finite difference for seismic wave extrapolation

Gang Fang, Qingdao Institute of Marine Geology, Jingwei Hu, Purdue University and Sergey Fomel, The University of Texas at Austin

SUMMARY

The lowrank finite difference (FD) methods have be obtained by matching the spectral response of the FD operator with the lowrank approximate recursive integral time-extrapolation (RITE) operator. We improve the accuracy and stability of lowrank FD method for first-order and second-order acoustic wave equation by using weighted least square (WLS). The weight function is designed according to the contributions of different wavenumber components to the accuracy of the FD scheme. After a stability analysis, we also introduce a taper constraint to restrain the FD operator to satisfy the stability condition. The numerical tests indicate that the proposed WLS-based lowrank FD scheme is accurate and stable for large time step seismic wave extrapolation.

INTRODUCTION

Wave extrapolation in time is an essential part of seismic imaging, modeling, and full waveform inversion. Finite-difference methods (Etgen, 1986; Wu et al., 1996) is one of the most popular and straightforward ways of implementing wave extrapolation in time. The finite-difference (FD) methods are highly efficient and easy to implement. However, the traditional FD methods are only conditionally stable and suffer from numerical dispersion (Finkelstein and Kastner, 2007).

The FD coefficients are conventionally determined through a Taylor-series expansion around the zero wavenumber (Dablain, 1986; Kindelan et al., 1990). Traditional FD methods are therefore particularly accurate for long-wavelength components. Several approaches have been proposed to improve the performance of FD method in practice. Implicit FD operators (Liu and Sen, 2009; Chu and Stoffa, 2011) can be used to achieve high numerical accuracy. Another way to control numerical errors is to use optimized FD operators (Takeuchi and Geller, 2000; Chu et al., 2009; Liu, 2013). Song et al. (2013) derived optimized coefficients of the FD operator from a lowrank approximation (Fomel et al., 2013) of the space-wavenumber extrapolation matrix.To improve the accuracy and stability and deal with the wave extrapolation of variable density, Fang et al. (2014) extend the lowrank FD methods on a staggered grid. Lowrank FD methods are accurate and stable than the usually used conventional FD methods. However, when using large time steps, wave extrapolation with lowrank FD methods still has numerical dispersion and sometimes will be unstable.

In this paper, we review the LS-based FD scheme for the first and second order wave equation. Then the WLS method is introduced to optimize the FD coefficients. We apply the stability analysis to the WLS-based FD scheme and design a taper function to improve its stability. We use lowrank decomposition to reduce the cost of optimizing FD coefficients. The numerical examples test the feasibility of the proposed method.

THEORY

WLS-based FD for second-order and first-order wave equation

We begin from the following second-order acoustic wave equation, which is widely used in seismic modeling and reverse time migration

$$\left[\frac{\partial^2}{\partial t^2} - A\right] p(\mathbf{x},t) = 0\,, \tag{1}$$

where $A = c^2(\mathbf{x})\nabla^2$, ∇^2 is the Laplacian operator and $\mathbf{x} = (x_1,x_2,x_3)$ is the space location. $p(\mathbf{x},t)$ is the seismic pressure wavefield, and $c(\mathbf{x})$ is the propagation velocity. Applying a second-order time-marching scheme and Fourier transform lead to the *kx*-space method (Tabei et al., 2002),

$$\frac{p(\mathbf{x},t+\Delta t) - 2p(\mathbf{x},t) + p(\mathbf{x},t-\Delta t)}{\Delta t^2} = c^2(\mathbf{x})\bar{\nabla}^2 p(\mathbf{x},t), \tag{2}$$

where $\bar{\nabla}^2$ is called pseudo-Laplacians (Etgen and Brandsberg-Dahl, 2009), which is defined as

$$\bar{\nabla}^2 p(\mathbf{x},t) = -\mathbf{F}^{-1}\left[\mathbf{k}^2 \mathrm{sinc}^2(c(\mathbf{x})|\mathbf{k}|\Delta t/2)\mathbf{F}[p(\mathbf{x},t)]\right]. \tag{3}$$

Another well-know expression for the wavefield extrapolation of equation 1 is the "two-step" marching algorithm

$$p(\mathbf{x},t+\Delta t) + p(\mathbf{x},t-\Delta t) = 2\Phi^2 p(\mathbf{x},t), \tag{4}$$

where Φ is the spatial pseudo-differential operator, which is defined as

$$\Phi^2 p(\mathbf{x},t) = \mathbf{F}^{-1}\left[\cos(c(\mathbf{x})|\mathbf{k}|\Delta t)\mathbf{F}[p(\mathbf{x},t)]\right]. \tag{5}$$

First-order wave equation is often used for the seismic wave extrapolation in a variable-density medium, which can be expressed in a vector form

$$\left[\frac{\partial}{\partial t} + B\right]\mathbf{u}(\mathbf{x},t) = 0\,, \tag{6}$$

where $\mathbf{u}(\mathbf{x},t)$ is a vector wavefield, $\mathbf{u}(\mathbf{x},t) = [\mathbf{v}(\mathbf{x},t), p(\mathbf{x},t)]^T$, $\mathbf{v}(\mathbf{x},t)$ is the acoustic particle velocity. B is defined as

$$B = \begin{bmatrix} 0 & \frac{1}{\rho(\mathbf{x})}\nabla \\ \rho(\mathbf{x})c^2(\mathbf{x})\nabla\cdot & 0 \end{bmatrix}. \tag{7}$$

Similar to the second-order *kx*-space method, equation 6 can be solved by first-order *kx*-space method on staggered grid

DOI http://dx.doi.org/10.1190/segam2015-5913120.1

(Song et al., 2012; Fang et al., 2014) by decomposing the pseudo-Laplacians into first-order pseudo-differential operator as

$$\bar{\nabla}^2 \equiv \left(\frac{\partial}{\partial^+ x}\frac{\partial}{\partial^- x} + \frac{\partial}{\partial^+ z}\frac{\partial}{\partial^- z} \right). \qquad (8)$$

The factored operators are given by (Fang et al., 2014), taking $\frac{\partial}{\partial^+ x}$ as an example

$$\frac{\partial p(\mathbf{x},t)}{\partial^+ x} \equiv \mathbf{F}^{-1}\left[ik_x e^{ik_x\Delta x/2}\mathrm{sinc}(c(\mathbf{x})\,|\mathbf{k}|\,\Delta t/2)\mathbf{F}[p(\mathbf{x},t)] \right]. \qquad (9)$$

The equation 3, 5, 9 provide space and wavenumber domain operators to calculate the wavefield. These mixed domain operators are also called recursive integral time-extrapolation (RITE) operator (Du et al., 2014), which allow simulating accurate wave extrapolation with little numerical dispersion.

Optimal FD schemes can be designed by fitting RITE operators in wavenumber domain. Following Song et al. (2013), define the finite difference scheme for the second-order spatial derivative as

$$D_1\left[p(\mathbf{x},t)\right] = \sum_{l=1}^{L} G(\mathbf{x},l)\left[p(\mathbf{x}-\Delta_L,t) + p(\mathbf{x}+\Delta_R,t)\right], \quad (10)$$

or for the first-order spatial derivative as

$$D_2\left[p(\mathbf{x},t)\right] = \sum_{l=1}^{L} G(\mathbf{x},l)\left[p(\mathbf{x}-\Delta_L,t) - p(\mathbf{x}+\Delta_R,t)\right]. \quad (11)$$

$G(\mathbf{x},t)$ is the FD coefficients, whose difference with the conventional FD coefficients is that $G(\mathbf{x},t)$ are changed with location $\mathbf{x}$. Δ_L and Δ_R are the space shift, which are defined as $\Delta_L = \Delta_R = (\xi_1(l)\Delta_1, \xi_2(l)\Delta_2, \xi_3(l)\Delta_3)$. For the standard grid, the $\xi_i(l), (i = 1,2,3)$ are integers provided the stencil information, $\xi_i(l) = 1,2,\cdots,L$. For the staggered grid, $\xi_i(l)$ can be half of the integers which indicated the points on half grid. Note that both the points on axis and off-axis can be used for the FD stencil. Considering the Fourier transform, the right side of the equation 10 and equation 11 can be expressed in wavenumber domain using a same form as

$$D\left[p(\mathbf{x},t)\right] = \mathbf{F}^{-1}\left[\sum_{l=1}^{L} G(\mathbf{x},l)B(l,\mathbf{k})\mathbf{F}\left[p(\mathbf{x},t)\right] \right], \quad (12)$$

where $B(l,\mathbf{k})$ is the base function, for the second-order spatial derivative $B(l,\mathbf{k}) = \cos(\sum_{i=1}^{3}\xi_i(l)\Delta_i k_i)$, for the first-order spatial derivative $B(l,\mathbf{k}) = \sin(\sum_{i=1}^{3}\xi_i(l)\Delta_i k_i)$. To obtained the FD coefficients $G(\mathbf{x},l)$, we use FD operator (equation 12) to approximate the RITE operator (equation 5 or 9) by the least square method

$$\min_G \left\| W(\mathbf{x},\mathbf{k}) - \sum_{l=1}^{L} G(\mathbf{x},l)B(l,\mathbf{k}) \right\|. \quad (13)$$

For second-order spatial derivative, $W(\mathbf{x},t) = \cos(c(\mathbf{x})|\mathbf{k}|\Delta t)$ is the kernel of equation 5, while for the first-order spatial derivative, $W_x(\mathbf{x},\mathbf{k}) = k_x\mathrm{sinc}(v(\mathbf{x})\,|\mathbf{k}|\,\Delta t/2)$ according to equation 9.

Note that in equation 13 the least square fitting is taken on the whole range of wavenumbers. Each wavenumber component's contribution to the fitting error is considered equally. However, the seismic signal is band-limited and its energy focuses on a small range around the dominant frequency. Thus, we introduce wavenumber weights for the least square fitting to make the wavenumbers close to the dominant frequency contribute more to the fitting error, while the wavenumber far away from the dominant frequency contribute less. With the wavenumber weight, equation 13 becomes

$$\min_G \left\| \bar{W}(\mathbf{x},\mathbf{k}) - \sum_{l=1}^{L} G(\mathbf{x},l)\bar{B}(l,\mathbf{k}) \right\|, \quad (14)$$

where $\bar{W}(\mathbf{x},\mathbf{k}) = w(k)W(\mathbf{x},\mathbf{k})$ and $\bar{B}(l,\mathbf{k}) = w(k)B(l,\mathbf{k})$, k is the value of the wavenumber. Here we take $w(k)$ an bimodal Gaussian weighted function as

$$w(k) = \frac{1}{2}\left[e^{-\frac{(k-k_0)^2}{a}} + e^{-\frac{(k+k_0)^2}{a}} \right], \quad (15)$$

where $k_0 = \frac{2\pi f_0}{c}$, f_0 is the dominant frequency of seismic signal. c is the velocity at the location point. Figure 1 shows two Gaussian weighted functions for $c = 4.5km/s$.

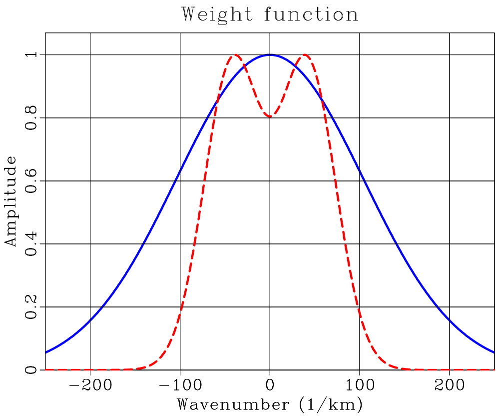

Figure 1: Gaussian weighted function. Blue solid line: $f_0 = 20Hz$, $a = 20000$. Red dashed line: $f_0 = 30Hz$, $a = 2000$.

Stability analysis

Next we provide the stability analysis for the proposed FD method. We take the WLS-based FD of first-order wave equation as an example. Since the RITE operators of first-order wave equation are more complicated than that of second-order wave equation, an similar stability analysis process can be easily applied to the WLS-based FD of second-order wave equation. From equation 14 we have following relation,

$$k_x\mathrm{sinc}(c(\mathbf{x})|\mathbf{k}|\Delta t/2)w(k) \approx \sum_{l=1}^{L} G(\mathbf{x},l)\sin\left(\sum_{i=1}^{3}\xi_i(l)k_i\Delta_i\right)w(k). \quad (16)$$

As the weight function is bounded between 0 and 1, we can

DOI http://dx.doi.org/10.1190/segam2015-5913120.1

ignore it and take a simple derivation

$$\sin(c(\mathbf{x})|\mathbf{k}|\Delta t/2) \approx \frac{1}{2}c(\mathbf{x})\Delta t\sum_{l=1}^{L}G(\mathbf{x},l)\sin\left(\sum_{i=1}^{3}\xi_i(l)k_i\Delta_i\right). \quad (17)$$

Because sin function is bounded, the right side of the equation 17 should have

$$-1 \le \frac{1}{2}c(\mathbf{x})\Delta t\sum_{l=1}^{L}G(\mathbf{x},l)\sin\left(\sum_{i=1}^{3}\xi_i(l)k_i\Delta_i\right) \le 1. \quad (18)$$

We will use Von-Neumanm stability analysis to prove that actually equation 18 is the stability condition of the FD scheme whose coefficients are given by $G(\mathbf{x},l)$. To simplify the derivations, we consider the 1D case of the first-order wave equation 6. Inserting the plane wave solution

$$\begin{aligned} u_m^n &= A_u e^{i(km\Delta-\omega n\Delta t)} \\ p_m^n &= A_p e^{i(km\Delta-\omega n\Delta t)} \end{aligned} \quad (19)$$

into the 1D discrete version of the equation 6, we have

$$\begin{bmatrix} u_{m+1/2}^{n+1/2} \\ p_m^{n+1} \end{bmatrix} = \begin{bmatrix} 1 & -i\frac{g}{\rho c}e^{ik\Delta/2} \\ -i\rho cge^{-ik\Delta/2} & 1-g^2 \end{bmatrix}\begin{bmatrix} u_{m+1/2}^{n-1/2} \\ p_m^n \end{bmatrix}, \equiv \Psi\begin{bmatrix} u_{m+1/2}^{n-1/2} \\ p_m^n \end{bmatrix} \quad (20)$$

where $g = 2\Delta tc\sum_{l=1}^{L}G(x,l)\sin(k\xi(l)\Delta)$. According to the Von-Neuman stability analysis, Ψ has

$$\|\Psi\| \le 1. \quad (21)$$

This indicates that Ψ's eigenvalues λ_i has

$$max|\lambda_i| \le 1. \quad (22)$$

The eigenpolynomial of the operator matrix Ψ is

$$\lambda^2-(2-g^2)\lambda+1=0. \quad (23)$$

From equation 22, we know that g need to satisfy

$$|g| \le 2, \quad (24)$$

which indicates that

$$-1 \le \frac{1}{2}c(x)\Delta t\sum_{l=1}^{L}G(x,l)\sin(\xi_i(l)k\Delta) \le 1. \quad (25)$$

For the 2D or 3D case, equation 18 is the stability condition of the FD scheme whose coefficients $G(\mathbf{x},l)$ are given by equation 14.

The FD operator equation 12 can be seen as a truncation of the RITE operator (equation 3, 8 or 9). The truncation error may make the FD operator overshoot the boundary when using larger time steps, which will cause the FD scheme unstable. We introduce a taper function to RITE operator to avoid instability of the FD scheme. The WLS problem to obtain optimal FD coefficients with the taper function $\tau(k)$ becomes

$$\min_G \left\|\tau(k)\bar{W}(\mathbf{x},\mathbf{k})-\sum_{l=1}^{L}G(\mathbf{x},l)\bar{B}(l,\mathbf{k})\right\|. \quad (26)$$

For a fixed $\mathbf{x}$, $\bar{W}$ is a smooth and oscillatory function about wavenumber $\mathbf{k}$. Thus the taper function should also be smooth and can automatically detect the value of $\mathbf{k}$, on which $\bar{W}$ shoot the threshold of stability condition. We design a taper function as

$$\tau(k) = \begin{cases} 1-\beta exp\left[1-\frac{1}{1-\left(\frac{k-k_0}{\alpha/2}\right)^2}\right] & , \quad if|k-k_0| \le \alpha/2 \\ 1-\beta exp\left[1-\frac{1}{1-\left(\frac{k+k_0}{\alpha/2}\right)^2}\right] & , \quad if|k+k_0| \le \alpha/2 \\ 1 & , \quad else \end{cases} \quad (27)$$

where k is the value from negative to positive Nyquist wavenumber. k_0 is the wavenumber which makes $\bar{W}$ shoot its boundary. Parameter α and β control the width and magnitude of the taper function. Figure 2 shows two different taper functions with $k_0 = 175$.

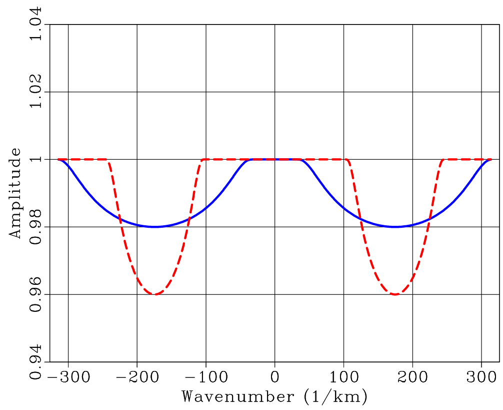

Figure 2: Taper function. Blue solid line: $\alpha = 300$, $\beta = 0.02$. Red dashed line:$\alpha = 150$, $\beta = 0.04$.

Lowrank approximation

We can obtain the FD coefficients $G(\mathbf{x},l)$ on each space location by solving the WLS problem defined with equation 26. However, for seismic extrapolation the number of the space location is huge. It is time-consuming to solve the WLS problem at each location points. We apply lowrank decomposition (Fomel et al., 2013) to the operator matrix $\bar{W}$ to save the computational cost of solving equation 26. Let us view the lowrank decomposition of $\bar{W}$ in matrix version,

$$\bar{W} \approx \bar{W}_1 A \bar{W}_2 \quad (28)$$

where $\bar{W}_1$ is the submatrix of $\bar{W}$ that consisted of the random picked n columns, $\bar{W}_2$ is the submatrix consisted of the random picked m rows. n and m depend on the rank of the matrix $\bar{W}$, which is much smaller than the number of the columns or rows of $\bar{W}$.

After applying lowrank decomposition, equation 26 can be described in a matrix version as

$$\tau\bar{W}_1 A\bar{W}_2 = G\bar{B} \quad (29)$$

DOI http://dx.doi.org/10.1190/segam2015-5913120.1

Since τ is depends on wavenumber, we have

$$\tau \bar{W}_2 = (\bar{W}_1 A)^{\dagger} G\bar{B}, \tag{30}$$

where $\dagger$ indicate the pseudo-inverse. Defining $C = (\bar{W}_1 A)^{\dagger} G$, we can find C by solving the WLS problem which constrained by the taper function τ

$$\tau \bar{W}_2 = C\bar{B}. \tag{31}$$

Then the FD coefficients G can be obtained by

$$G = \bar{W}_1 A C. \tag{32}$$

Once we have the FD coefficient from equation 32, the seismic wavefield can be extrapolated by the FD scheme. Because this FD method is based on a WLS fitting and is the extension of lowrank FD methods (Song et al., 2013; Fang et al., 2014), we call this new method *WLS-based lowrank FD* method.

Numerical examples

In this section we use numerical examples to verify the feasibility of the WLS-based lowrank FD method. We consider a 1D model contains a quadratic increase in velocity, $c(x) = 1.7 + 0.02x^2$, which if from $1.7km/s$ to $3.6km/s$. The space interval Δ is $10m$ and time interval $\Delta t = 4ms$. A Ricker wavelet point source with dominant frequency of 20 Hz is used for seismic extrapolation.

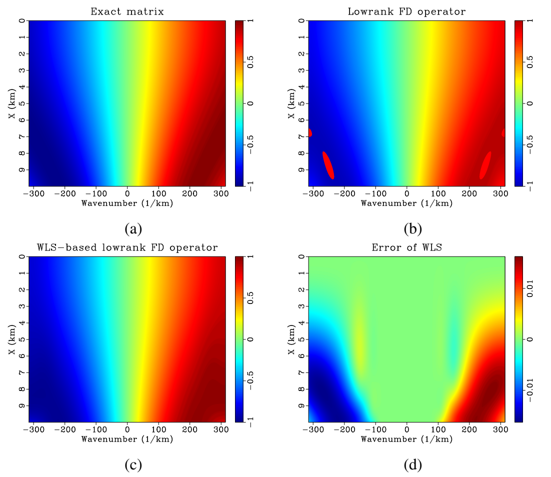

Figure 3: (a) The exact operator for 1D quadratic increasing velocity. (b)Lowrank FD operator. (c) WLS-based lowrank FD operator. (d) Error of WLS-based lowrank FD operator.

Figure 3a shows the exact RITE operator. Figure 3b shows the lowrank FD operator. Generally, lowrank FD method is accurate and stable. But when the time interval is large or the velocity variation is rapid, the lowrank FD method may become unstable. The red patches shown in figure 3b indicate the area where the operator overshoots its stability condition. As shown in figure 3c, the WLS-based lowrank FD, which include a taper to constrain its stability, avoids the operator overshooting the boundary -1 and 1. Figure 3d show the error of WLS-based lowrank FD operator. We can see the error is mainly concentrated on the high wavenumber part.

Figure 4a and 4b show the wave propagation with lowrank FD and lowrank FD with WLS. Since we use large time step, the propagation is unstable. Figure 4c shows the wavefield of lowrank FD method with taper constraint. We can see because of the taper, the wavefield propagation is stable, although the numerical errors become serious when propagation time goes on. From figure 4d, we can see that when use lowrank FD with WLS and taper constraint, the wavefield propagation is stable and the error are effectively suppressed.

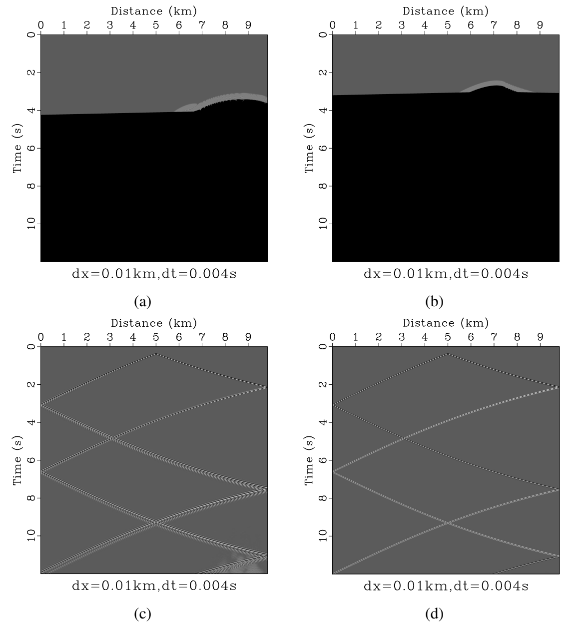

Figure 4: Wavefield generated by (a) lowrank FD method, (b) lowrank FD with WLS (c) lowrank FD method with taper constraint, (d) lowrank FD with both WLS and taper constraint.

CONCLUSIONS

The WLS-based lowrank FD method is proposed for seismic extrapolation. An bimodal Gaussian weighted function is used for the LS fitting to increase the accuracy of the FD method, while an taper function is introduced to improve its stability. The stability analysis indicates that the stability condition of the FD scheme is defined by the mix domain RITE operator. The WLS-based lowrank FD method can be used to solve the second-order wave equation as well as the first-order wave equation. 1D numerical examples show the feasibility of the new method for the wave extrapolation with large time steps. The 2D implementation is in process, which will be shown in the annual meeting.

ACKNOWLEDGMENTS

We thank all developers of the Madagascar open-source software package (http://ahay.org). This paper will also be reproducible by Madagascar.

DOI http://dx.doi.org/10.1190/segam2015-5913120.1

EDITED REFERENCES

Note: This reference list is a copyedited version of the reference list submitted by the author. Reference lists for the 2015 SEG Technical Program Expanded Abstracts have been copyedited so that references provided with the online metadata for each paper will achieve a high degree of linking to cited sources that appear on the Web.

REFERENCES

Chu, C., and P. L. Stoffa, 2011, Application of normalized pseudo-Laplacian to elastic wave modeling on staggered grids: Geophysics, **76**, no. 5, T113–T121. http://dx.doi.org/10.1190/geo2011-0069.1.

Chu, C., P. L. Stoffa, and R. Seif, 2009, 3D elastic wave modeling using modified high-order time stepping schemes with improved stability condition: 79th Annual International Meeting, SEG, 2662–2666.

Dablain, M. A., 1986, The application of high-order differencing to the scalar wave equation: Geophysics, **51**, 54–66. http://dx.doi.org/10.1190/1.1442040.

Du, X., P. Fowler, and R. Fletcher, 2014, Recursive integral time-extrapolation methods for waves: A comparative review: Geophysics, **79**, no. 1, T9T26.

Etgen, J., 1986, High-order finite-difference reverse-time migration with the two way nonreflecting wave equation: SEP-48, 133–146.

Etgen, J., and S. Brandsberg-Dahl, 2009, The pseudo-analytical method: application of pseudo-Laplacians to acoustic and acoustic anisotropic wave propagation: 79nd Annual International Meeting, SEG, Expanded Abstracts, 2552–2556.

Fang, G., S. Fomel, Q. Du, and J. Hu, 2014, Low-rank seismic wave extrapolation on a staggered grid: Geophysics, **79**, T157–T168.

Finkelstein, B., and R. Kastner, 2007, Finite-difference time domain dispersion reduction schemes: Journal of Computational Physics, **221**, no. 1, 422–438. http://dx.doi.org/10.1016/j.jcp.2006.06.016.

Fomel, S., L. Ying, and X. Song, 2013, Seismic wave extrapolation using low-rank symbol approximation: Geophysical Prospecting, **61**, no. 3, 526–536. http://dx.doi.org/10.1111/j.1365-2478.2012.01064.x.

Kindelan, M., A. Kamel, and P. Sguazzero, 1990, On the construction and efficiency of staggered numerical differentiators for the wave equation: Geophysics, **55**, 107–110. http://dx.doi.org/10.1190/1.1442763.

Liu, Y., 2013, Globally optimal finite-difference schemes based on least squares: Geophysics, **78**, no. 4, T113–T132.

Liu, Y., and M. K. Sen, 2009, An implicit staggered-grid finite-difference method for seismic modeling: Geophysical Journal International, **179**, no. 1, 459–474. http://dx.doi.org/10.1111/j.1365-246X.2009.04305.x.

Song, X., S. Fomel, and L. Ying, 2013, Low-rank finite differences and low-rank Fourier finite-differences for seismic wave extrapolation: Geophysical Journal International, **193**, no. 2, 960–969. http://dx.doi.org/10.1093/gji/ggt017.

Song, X., K. Nihei, and J. Stefani, 2012, Seismic modeling in acoustic variable-density media by Fourier finite differences: Presented at the 82nd Annual International Meeting, SEG.

Tabei, M., T. D. Mast, and R. C. Waag, 2002, A k-space method for coupled first-order acoustic propagation equations: The Journal of the Acoustical Society of America, **111**, no. 1, 53–63. http://dx.doi.org/10.1121/1.1421344.

Takeuchi, N., and R. J. Geller, 2000, Optimally accurate second order time-domain finite difference scheme for computing synthetic seismograms in 2D and 3D media: Physics of the Earth and Planetary Interiors, **119**, no. 1–2, 99–131. http://dx.doi.org/10.1016/S0031-9201(99)00155-7.

Wu, W., L. R. Lines, and H. Lu, 1996, Analysis of high order, finite-difference schemes in 3D reverse-time migration: Geophysics, **61**, 845–856. http://dx.doi.org/10.1190/1.1444009.

DOI http://dx.doi.org/10.1190/segam2015-5913120.1